Budapest University of Technology and Economics
Faculty of Transportation Engineering and
Vehicle Engineering

Investigation of structured surfaces of automotive tools by modifying micro- and macro-geometric properties

Ph.D. dissertation booklet

Author:

Krisztián Kun

mechanical engineer

Supervisors:

Zoltán Weltsch Ph.D.
associate professor

János Líska Ph.D.
college associate professor

Budapest
2023

Table of contents

1. Introduction

In the automotive industry, the expectations for plastic products are getting higher and higher in terms of aesthetics, surface finish, dimensional accuracy and increasing mechanical properties. Numerous raw material developments and special processing technologies are being brought to light, thus keeping injection moulding a constantly developing and leading sector in this segment of the industry.

Increased customer demand makes the quality of plastic parts an increasingly important issue. [1] In injection moulding, the exact effect of processing parameters and thermal phenomena on the filling of the desired micro surfaces is not known. However, producing a quality product requires perfect knowledge of the cavity filling process. [2]

Microstructures created on the surface of polymer products can not only have an aesthetic but also a functional role. When creating stiffening rib-like microstructures on the moulding surface, they can alter the shear stress during injection moulding. The melt gets oriented on the area of the structures. The created surfaces also increase the inertia of the product cross-section. Changing the moulding surface can therefore affect the stiffness of the product due to its material structure and geometry.

The aim of the research is to create functional surface structures on the moulding surface of an injection moulding tool using femtosecond laser technology (which is in the process of significant development in automotive applications) and studied their effects. I performed two sequential series of experiments in which microstructures were created on the moulding surface of test injection moulding tools using laser. In the first series of experiments, I investigated the effect of the orientation of the structures relative to the melt front, while in the second series I investigated the effect of their depth.

The aim is to provide results of scientific and industrial value to demonstrate the influence of the modified mould surface on the flow of the polymer melt - and thus on the filling of the surfaces - and on the mechanical properties of the injection moulded products. The raw materials used are automotive polypropylenes and their recycled and carbon nanotube reinforced versions.

2. Literature review

In my research, in accordance with the development trends of the automotive industry, I used the most widely used production process, injection moulding, and the most processed raw material in terms of volume, polypropylene (PP). However, my aim was not to develop raw materials, but to investigate the relationship between the moulding surface of the injection mould and the polymer melt. [3]

2.1. Creating surface microstructures in practice

The term microstructure according to the standard [4] is also used in polymer technology, with a size range from 1 μm to 100 μm according to the literature available. However, B. Sha et al. in their study referred to microstructures as surface area units below 200 μm. [5]

Structures can not only have an aesthetic function, but can also modify the mechanical properties of the product. They can be created using numerous manufacturing technologies. [6]

The use of femtosecond lasers can be advantageous in industrial environments compared to other surface treatment processes because:

- Micro-machining's biggest drawback, complex tool geometry design and tool wear, is eliminated.
- Compared to photochemical etching, it does not require chemicals and other consumables thus does not produce hazardous waste.
- More favourable than other thermal processes, as the heat affected zone is negligible.
- Compared to micro-spark eroding, the machine time for the process is significantly less. [7], [8]

In their research, Calabrese L. et al. showed that the process could be an alternative to thermal energy-based manufacturing methods such as electro-erosion or chemical energy lithography. [9]–[14]

2.2. The formation of microscopic surfaces

Injection moulding is also a key technology in the mass production of microstructured parts, due to its low cost per product, thus allowing for industrial scale volumes. The microstructures formed on the surface of polymer products are created by mapping the moulding surfaces, thus we can talk about surface replication. The quality of parts with structured surfaces can be affected by numerous parameters.

In their research, Uffe Arlø Theilade and Hans Nørgaard Hansen found that temperature is an important factor during replication, as increasing the temperature of the melt increased the filling of microstructures by almost twofold. A similar change in height is observed when the injection rate is increased. [17]

Attia U. et al. in a research summary pointed out the phenomenon that high tool temperatures can reduce the thickness of the solidified layer and delay the cooling of the cavity, allowing more material to enter the microstructures. Referring to several published results, the researchers defined the term "material hesitation" to refer to the effect where the melt enters the structured tool cavity at high velocity, then skips the microstructures and "flows over" them. These unfilled areas could only be mapped by the melt at the end of the injection phase, due to the backpressure. [18]–[20]

B. Sha, S. Dimov, C. Griffiths and M.S. Packianather investigated the formation of microscale shapes. PP base material has been found to form so-called rings, which can be explained by the fact that the material "hesitates", i.e. stops temporarily and fills the micro-surfaces only after the final cavity pressure is reached. The phenomenon leads to solidification of the outer layer of the melt, while the melt stream continues to flow inwards. Counterbalancing this by increasing the injection rate and the melt temperature, they were able to inject more melt before reaching the maximum cavity pressure. [5]

Chang H. and Young W. found that by changing the cooling time, the rate of shrinkage can be significantly altered. [21]

Yokoi H. et al. defined the TR (Transcription Ratio) factor as a measure of the quality of filling in their study. The TR factor, which measures the goodness (quality) of the moulding, essentially compares the depth of the structure formed on the mould with the maximum height of the surface moulded on the product. In their study, the researchers made the important finding that although previous results have suggested that the significant factors in microstructure imaging are temperature-related (melt and mould temperature), their hypothesis is limited by material degradation and the fact that higher mould temperatures mean longer cooling times and therefore longer cycle times.

2.3. The mechanical properties in realition to micro-surface structures

In their research, Pantani R. et al. showed that during the injection moulding process there is always some degree of molecular orientation, which varies in the cross-section of the moulded product. [22] Yin J. et al. demonstrated with their measurements that during injection moulding process, when polymer melt flows in a closed cavity (mould insert), the velocity of the layers near the wall will be lower than that of the layers in the centre of the cavity due to friction. [23]

In the scientific report of Belina K., he pointed out that, due to the velocity profile, the orientation rate is higher near the wall than in the middle of the cavity. In the process, layers are deposited on the mould wall, which cools further. The layers next to the wall is elongately oriented. The shearing action between layers that are still in the melt state and already solidified creates the sheared oriented layer, and then, moving towards the middle of the product, we find less oriented or unoriented layers. [2] Due to these effects, a complex shell-core structure is formed in the injection moulded specimens, which can be adjusted by processing parameters and influenced by surface structures. [24]

C. Gomik has also studied the flow conditions of injection moulding tools with microstructured surfaces. In his work, he noted that the plug flow near the tool wall results in highly oriented layers due to the higher shear rate. However, the formation of layers can be affected by the influence of microstructures on the melt front. [25]

Porfyrakis K. et al. investigated the relationship between processing parameters, microstructured mould surface and mechanical properties in poly(methyl methacrylate) (PMMA) based test specimens. It has been found that due to the surface microstructures ("ridges"), the material flow pressure and shear stress increases. The injected material is oriented on the face of the surface structures. The change in the shaping surface has affected the flow pattern of the melt, and the larger surface area allows more heat to be introduced into the system through the heated mould, resulting in less solidification along the cavity. [26]

In a scientific publication, Solomon N. and his research colleagues investigated the filling of automotive parts with a structured surface (leather effect) made of PP material by injection moulding using a complex experimental design. Out of all the factors studied, the injection rate had the greatest effect on the quality of the filling, followed by about half the influence of the mould temperature and the change in the temperature of the molten plastic. [27]

In all of the literature sources detailed, researchers have used unrecycled, so-called original material. Recycling causes a significant change in the morphological structure of the material. It is generally the molecular chain or the crystalline structure that is damaged. Their negative effect is the deterioration of mechanical properties. [28], [29] To restore the physical properties of the original material as indicated in its data sheet, the automotive industry is increasingly using carbon nanotubes (CNTs) in addition to glass and carbon fibre alloys to produce nanocomposites.

2.4. Effect of carbon nanotubes in PP/CNT nanocomposites

In their research, Grimmer C. and Dharan C. combined the reinforcing phases, a glass fibre reinforced PP base material with an additional 1 m/m% CNT content. Upon testing the fatigue of the specimens, they found at least 60% improvement due to the carbon nanotube reinforcement. [30]

In a study by Ashok Gandhi R. and colleagues, the effect of CNT content on the hardness of PP/CNT composites is described. In their research they investigated the properties of PP/CNT composites containing 1, 3, 5 and 7 m/m% of CNT. Hardness is an important mechanical property that determines the applicability of polymer composites. Based on the researchers' results, the hardness of the PP/CNT composite increases significantly with increasing CNT ratio in the PP matrix. It is worth pointing out the high CNT weight ratio, which in this case also resulted in a considerable increase in costs. [31]

Zhang et al. found in their publication that the MFI of raw feedstock decreased dramatically from 33 g/10 min to 0.84 g/10 min with the addition of 5 wt% CNT, and then stagnated with further increase in the weight percentage of the reinforcing phase. It is worth noting that, based on the curve plotted according to the standard, the change in MFI below 1 m/m% CNT was still negligible. Recyclation led to chain breakage, degradation of the material, and thus an increase in MFI: 14-fold recyclation resulted in a nearly threefold increase in MFI to 90 g/10 min in comparison to the original material. In contrast, recycling the 3 m/m% CNT feedstock 14 times has taken the feedstock to its original value of about 33 g/10 min.

With regard to the impact strength, it was found that the original raw material and the 3 m/m% PP/CNT composite showed almost identical values up to 10-fold recyclation. Recycling over 10 times, however, has significantly degraded the raw polymer, while the reinforced specimens still yielded the previous values. Based on this phenomenon, carbon nanotubes in the polymer matrix not only increase the mechanical properties but also improve the recycling resistance. [32], [33]

2.5. Critical Evaluation of the Literature

Based on the literature review, it can be said that, the available scientific results discuss:

1. **Micromachining of the moulding surfaces** with femtosecond lasers might be preferable in comparison to other structuring processes in industrial environments. [14], [34]–[36]
2. The quality of **surface structures on injection moulded products** is influenced by process parameters. [5], [25], [26], [37]–[39]
   - The extent of their effect is not consistent in the literature.
   - Technology recommendations in this field are needed.
3. Surface structures can change the number and proportion of **orientation layers** in the injection moulded product. [23], [24], [26]
   - However, the scientific results on the relationship between mechanical properties and micro-surface structures are incomplete.
4. **The presence and position of micro-surfaces** influence the flow of the melt front and, through this, the quality of the end product. [40], [41]
   - The quality of the infill can be described by the TR-factor.
   - The effect of the orientation of the micro-surfaces relative to the melt front on the mapping of the end product requires knowledge of the infill.
   - Knowledge of the influence of structure depth and orientation on the behaviour of mechanical properties is lacking in scientific results.
5. There is a scarcity of scientific results on the effect of recycling and the changes in flow index and mechanical properties caused during the reinforcement phase in **CNT-reinforced polypropylene nanocomposites**. [32], [33], [42]
   - However, the relationship between the microstructures formed on the shaping surfaces and the carbon nanotube reinforced materials in terms of neither filling nor mechanical property changes is not defined in the literature.

3. Aim of research

Based on the literature review, **the hypotheses** that the orientation and depth of microstructures made of polypropylene material that replicated laser surface treatment influences the flow of the melt. The increased mould surface area affects the cooling and heat transfer conditions and can change the proportion of oriented layers in polymer products. The mechanical properties of plastic products can be caused by the influence of microstructures on the core-shell structure.

As a result, it can be assumed that:

- The mapping of structured surfaces can be significantly increased by optimally adjusting the significant factors. [5], [25], [26], [37], [38]
- Process parameters of injection moulding and correlation of microstructures formed on the surface have varying influence on the flexural strength and impact strength.

Test specimens moulded from recycled carbon nanotube reinforced polypropylene material affect the flow properties of the melt in proportion to the weight percentage of the reinforcing phase. The surface area increased by the structures affects the cooling and heat transfer conditions and may change the ratio of layers with different orientations.

As a consequence, it can be assumed that:

- Products with structured surfaces made from recycled PP base material containing CNTs can have their fill factor increased by optimum adjustment of the significant factors. The filling factor is influenced by the change of the flow index and the mass percentage of the reinforcing phase. [25], [37], [38]
- Recycled polypropylene reinforced with low wt% (0.1 - 0.5 wt%) carbon nanotubes, during injection moulding, the shaping surfaces influence the storage modulus values measured on the finished product. [32], [33], [42]

3.1. Research plan and objectives

As noted in the hypotheses, two closely related trends appear somewhat separate (Figure 1). The solution of these problems was also carried out successively over time due to the complexity of the research area. As a result, two series of experiments were carried out, focusing on the following areas:

1. **series of experiments:** the effect of microstructure orientation on the formation and mechanical properties of specimens made from a high flow polypropylene combined with random copolymer.
2. **series of experiments:** the effect of microstructure depth on the formation and mechanical properties of the produced specimens using polypropylene block copolymer and recycled PP/CNT nanocomposite materials.

The test pieces are manufactured using a special experimental injection moulding tools, the products of which have standard shapes. On the mould surface, I create surface structures in specific directions and at different depths according to the orientation of the melt flow. The structures are formed using a femtosecond laser.

Following micro-surface structuring, I use mould inserts to produce experimental test specimens using injection moulding with automotive grade materials. I begin the tests (to determine the base values) by analysing the structures created on the tool inserts. Thereafter, using the moulding inserts specified by the complex experimental plan, the evaluation of the formation quality of the structures on the surface of the test specimens, drawing conclusions based on the measurements and making industrial recommendations will be carried out.

Since the topology of the moulding surface has a significant influence on the filling and the efficiency of heat transfer, it can be assumed that the core-shell structure is altered, thus changing the mechanical properties of the products. [23], [24], [26] Following the geometrical investigations, I will evaluate the measurements of the mechanical properties of the products, and make conclusions and observations based on the results, and propose industrial applications.

A brief summary of the research stages:

I. Laser structuring of injection moulding tool insert → **II.** Investigating the quality of the surface treatment → **III.** Injection moulding → **IV.** Examination and evaluation of the replicated microstructures → **V.** Measurement and evaluation of mechanical property changes caused by microstructures.

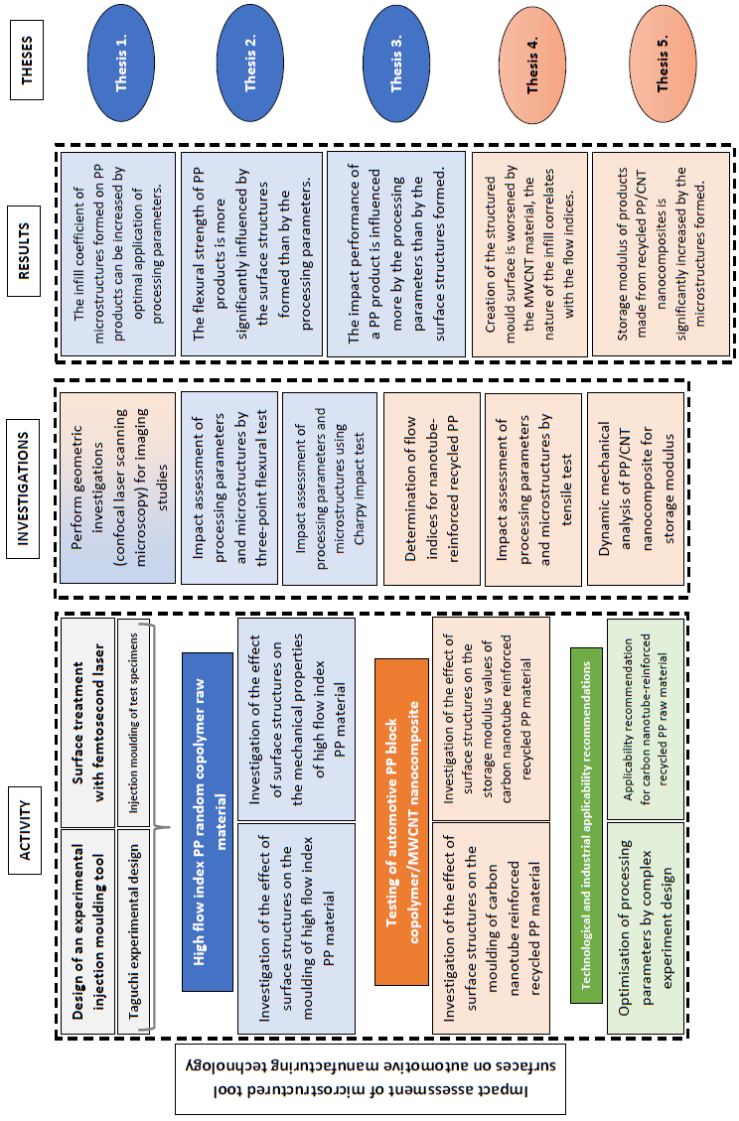

FIgure 1. The complex research plan leading to theses

4. Experimental materials, equipment and procedures

The research involved two series of experiments, built on each other. This chapter discusses the technological conditions and necessary details used in the experimental series. The surface structure of the tool insert was formed using a Coherent Monaco 1035-80-40 femtosecond laser. [43]

4.1. The structured insert used for the first set of experiments

In the first set of experiments, I carried out an impact assessment of the moulding surface for my self designed and manufactured injection moulding tool. Based on the literature available, the experiments focus on the following areas:

"*Influence of microstructure orientation* on the replication and mechanical properties of test specimens manufactured from a high flow polypropylene random copolymer."

Parallel and perpendicular groove geometries (micro-grooves) have been created. Models illustrating the geometries are shown in Figure 2.

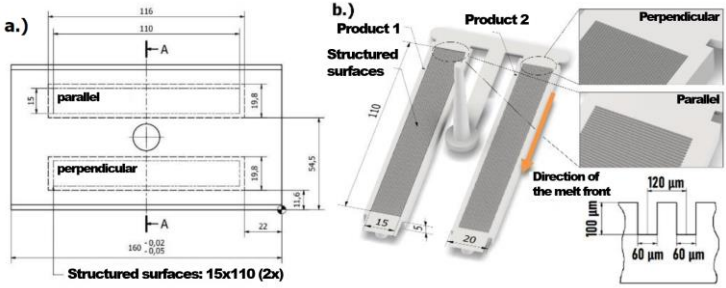

Figure 2. The structured insert designed for the first set of experiments a.) and its product b.)

As a reference, the stationary side insert was also produced with a grinded surface without laser surface treatment. With a surface roughness of Ra=0,4 µm. The grinding was done on a TOS BM102 tool grinder, the surface was measured on a SV-C3000 contour measuring machine. The parameters of the femtosecond laser used for structuring are given in Table 1.

Table 1. Parameters for femtosecond laser surface treatment

Average performance	15 W (25%)
Energy	20 μJ
Frequency	188 kHz
Wavelength	1035 ± 5 nm
Pulse length	277 fs
Mode	TEM_{00}, (M^2 < 1,2)
Scanning speed	5 m/s
Scanning repetitions	30 x
Applied surface treatment strategy	point (10 pulses/point)

4.2. The structured insert used for the second set of experiments

In the second series of experiments, I investigated the filling of mould surfaces and the change in mechanical properties of the test specimens using automotive-grade polypropylene and its recycled and carbon nanotube reinforced versions. Therefore, the focus of the second series of experiments is:

"*Influence of microstructure depth* on the deposition and mechanical properties of manufactured specimens from polypropylene block copolymer and recycled PP/CNT nanocomposite materials."

The specimens were manufactured using a standard tensile test piece injection moulding tool modified to suit the research. During the modification, I designed additional inserts for the tool in the B-side mould cavity (Figure 7).

Three types of inserts were made:

- Ground inserts without laser surface treatment (2 pcs),
- 20 μm deep micro grooved inserts with parallel flow lines (2 pcs.),
- 100 μm deep micro grooved inserts with parallel flow lines (2 pcs.).

The injection moulding cavity (Figure 3) contained two temperature and pressure sensors in the A-side, at the inlet section of the cavity. [44]

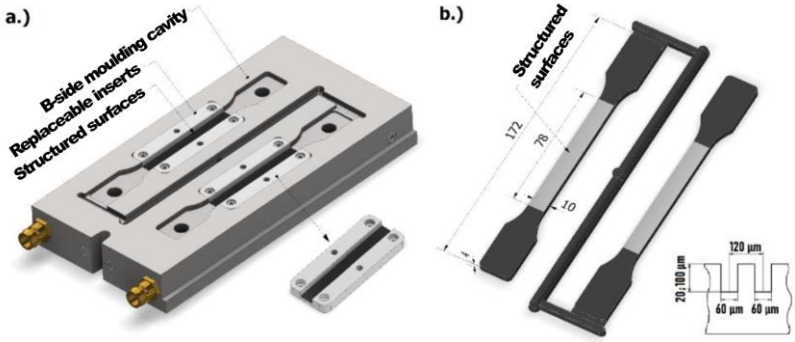

Figure 3. Moulding insert (a.) and moulding product (b.) designed for the second set of experiments

In the first set of experiments, the laser surface treatment took longer than expected, so in order to make the pattern creation more applicable to industrial applications, I changed the technological parameters in the second set of experiments, which are shown in Table 2.

Table 2. Parameters of the femtosecond laser surface treatment used in the second set of experiments

Average performance	24 W (40%)
Energy	32 µJ (at 750 kHz)
Frequency	750 kHz
Wavelength	1035 ± 5 nm
Pulse length	277 fs
Mode	TEM_{00}, (M^2 <1,2)
Scanning speed	5 m/s
Scanning repetitions (20 µm)	100 x
Scanning repetitions (100 µm)	500 x
Applied surface treatment strategy	line

4.3. Material used for the first set of experiments

In the first series of trials, the test samples were made from a product developed by MOL Petrochemicals and SLOVNAFT, called TATREN RM 85 82 CLEAR. Polypropylene random copolymer base material suitable for filling products with microstructured surfaces, as it is characterised by a high melt flow index (MFI) and excellent processing stability. [45]

4.4. Materials used for the second set of experiments

In the second series of experiments, in order to make the results applicable to the automotive industry, I used a specially developed Tipplen K 499 block copolymer polypropylene [46] as a raw material, as well as a carbon nanotube (PLASTICYLTM PP2001 MWCNT) [47] reinforced, recycled version of the same polypropylene with different weight percentages of reinforcement phase. The base polypropylene without CNT reinforcement phase, which has not yet been recycled, is referred to as the original raw material. The blend is 5-fold thermomechanically stressed a recycled nanocomposite containing 0.1 m/m% and 0.5 m/m% CNT.

4.5. Production of test specimens based on DOE

I used a Wittmann Battenfeld Ecopower 55 machine for the injection moulding of the test specimens in both sets of experiments. [48]

The special injection mould produced **for the first series of experiments** contains two symmetrically positioned mould cavities. In the Taguchi experimental design, I used three variables (so-called factors) which, according to the literature, have a significant effect on both the filling and the structure of the final product.

The factors tested are the injection rate (56, 80, 104 cm^3/s), the backpressure (245, 350, 455 bar) and the cooling time (20, 30, 40 s). The experimental design was created using Minitab software.

The tool used **in the second series of experiments** was equipped with a special sensor system, which allowed the determination of a stable range of injection velocities (90 cm3/s). Other constants were mould temperature 40°C, cooling time 40 s, as recommended in the original material's data sheet (Tipplen K 499 PP) [46].

Since the definition of the melt temperature was also specified in the datasheet as a range (190 – 230°C), I defined the melt temperature as a range of three variables (190, 210 230°C). The value of the backpressure was also specified as a variable at three levels (200, 500, 800 bar), as recommended in the literature, thus creating a two-factor three-level experimental design for the second set of experiments.

4.6. Description of examination procedures

After production, the specimens were subjected to geometrical and mechanical-strength characterisation in the laboratories of the John von Neumann University.

4.6.1. Microscopic examinations

During the geometric tests I measured the surface of the mould insert and the injection moulded specimens using conventional and confocal microscopes. I used an Olympus GX41 as a conventional light microscope to set up the laser surface treatment technology. Using the Olympus LEXT5100 confocal microscope [49], my aim is to investigate the results of laser surface treatment on the moulding surface of the injection moulding tool and the TR ("transcription ratio") of the polymer specimens produced with the mould. [41] With the confocal microscope used, the accuracy required for the analyses was feasible. The 3D point clouds measured by the microscope were compared with the designed geometry using Autodesk Inventor software. To represent the 3D topology, I used a freeware tool called Gwyddion.

4.6.2. Determination of the melt flow index (MFI)

Melt flow index (MFI) was determined according to ISO1133 using an Instron CEAST MF20 Modular Melt Flow Index Meter. The applied load according to the standard is 2,16 kg.

4.6.3. Three-point bending test

The three-point bending was carried out on an Instron 3366 universal mechanical materials testing machine in compliance with MSZ EN ISO 178. I set the distance between the supports to 64 mm. The crosshead speed was 5 mm/min. The maximum deflection was set at 15 mm, where the specimens had not yet broken.

4.6.4. Charpy impact test

I conducted the impact tests in the first series of experiments on the test specimens. The Charpy impactor used is an Instron Ceast Impactor II materials testing instrument, on which a 5 J impact hammer was used for the measurements. Using an Instron Ceast motor-driven notching machine, V-shaped notches of 1 mm depth were made on the test specimens.

4.6.5. Tensile test

The tensile test was carried out with specimens with a structured surface prepared for the second series of experiments according to MSZ EN ISO 527. Tensile testing was carried out on the Instron 3366 material testing machine, also used for bending, with sliding vises. Crosshead speed was set to 50 mm/min.

4.6.6. Dynamic Mechanical Analysis - DMA test

Test method for dynamic mechanical analysis with the TA Instruments Q800: three-point bending, set frequency 1 Hz, bending aplitude 15 μm, test temperature -10 – 100°C.

5. Results and evaluation

I examined the results of the two sets of experiments separately, component by component. The presentation of the results is the same for both sets of experiments: first the geometric measurement of the mould insert, then the quality of the moulding, and then the impact of the surface structures on the mechanical properties were evaluated.

5.1. Evaluation of the result of the first set of experiments

In the first set of experiments, I investigated the effect of the directions of the microstructures relative to the melt front. During the tests, the measured values of the structured polymer products were compared with the measured values of the specimens representing the surface of the ground tool insert. In the first step, I evaluated the exact geometry of the surface to be replicated, against which the quality of the filling of the moulded products could be measured. I then evaluated the quality of the replication and the effect of the surface structures on the bending and impact strength.

5.1.1. Results of laser surface treatment on the mould insert

The laser machining parameters were the same for the production of micro-slots formed parallel and perpendicular to the flow of the polymer melt. The depth of the designed structures was 100 μm, however, the depth of the actual measured geometry is the relevant depth for moulding. The 3D topologies generated in Gwyddyon from the data set captured by the microscope are shown in Figure 4. With the help of the software, it was possible to determine the actual (average) depth of the grooves made in the mould insert. In practice, the grooves with a planned depth of 100 μm were found to have an average depth of 79 μm for parallel structures and 73 μm for perpendicular structures. This provided the baseline for the filling investigation in the first set of experiments. The formed macro- and micro-geometrical features (the structure profile) were influenced by the laser beam source. The laser beam used a TEM_{00} mode, which causes the intensity distribution of the beam to follow a Gaussian distribution. This is also visible in the geometries formed.

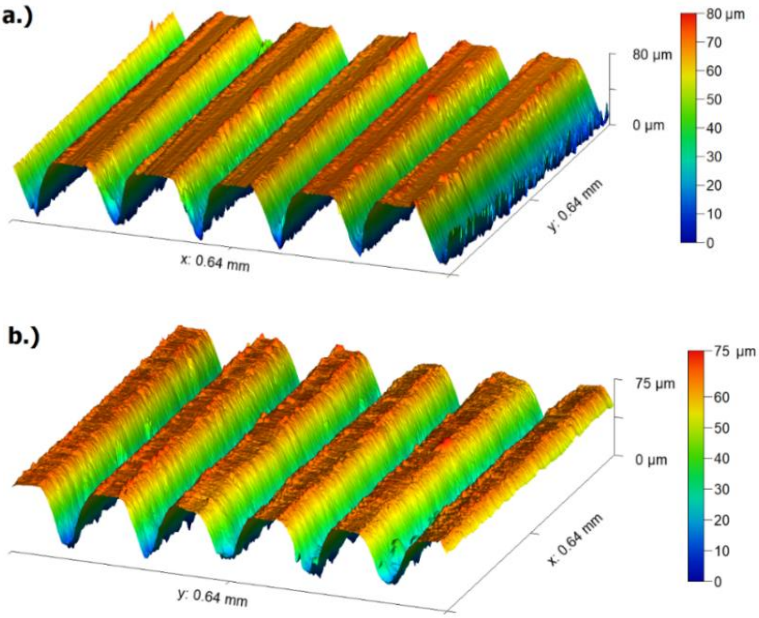

Figure 4. 3D topology of a tool insert structured with parallel (a.) and perpendicular (b.) grooves created in Gwyddion software

The difference in size (5 µm on average) and quality between the two surface treatments was caused by heat build-up, i.e. the laser beam spent more time in a small area of the insert due to the short paths when producing perpendicularly structured surfaces, so heat dissipation could not be as fast. In contrast, for parallel (longitudinal) paths, heat dissipation was more consistent.

As presented in the literature [41], the moulding goodness factor TR essentially compares the depth of the tool groove to the maximum height of the moulded surface. To do this, I used a cross-sectional sketch of the model to create the surface profile of the insertsSince the perpendicular and parallel structures showed different depths, the amount of residual material caused variations in the surface area of the insert and, through it, the manufactured product (Figure 5). **The perpendicularly structured insert increased the surface area of the part produced with it by 33%, the parallel one by 36%.**

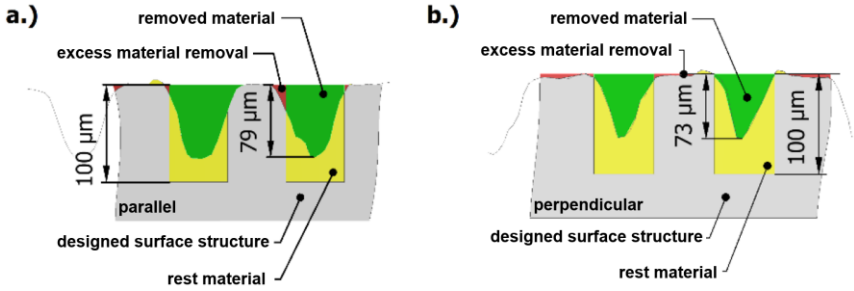

Figure 5. Differences between designed and machined surfaces: for parallel (a.) and perpendicular (b.) structured surface

5.1.2. Results of injection moulded specimen replication

In the mapping tests of the moulding inserts, I used the TR-factor to assess the quality of the maoulding according to the literature. The better the TR factor, the closer the height of the ridge formed on the polymer product approximates the depth of the structure on the insert. The TR-factor is expressed in percentage to make it easier to understand. By fitting a trend line to the point set and then plotting its equation, a mathematical model approximating the filling can be formulated. The measurement points are well approximated by linear trend lines (R2>90%), illustrated in Figure 6.

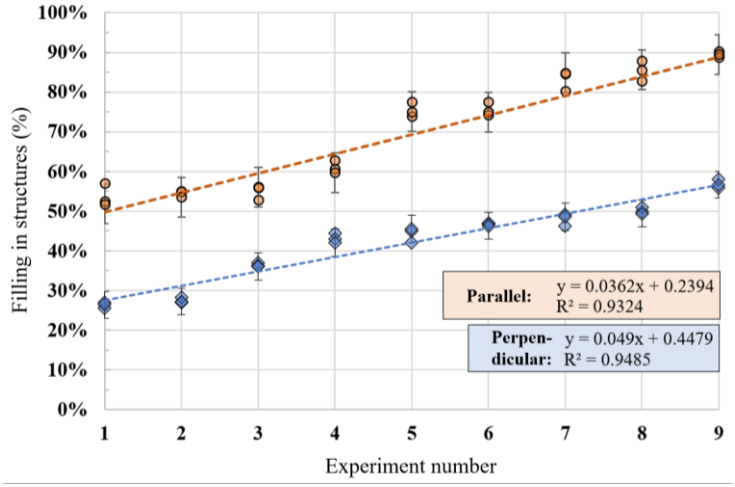

Figure 6. Quality of filling of structured products

As a result of the experimental study, it can be concluded that by increasing the injection moulding rate when using PP as a base material, which is used in large quantities in the automotive industry, the deposition can be significantly increased for the structures investigated.

The orientation of the formed micro-slots with respect to the melt front had an opposite effect on the filling: in all the experiments studied, the TR coefficients of the specimens having parallel and perpendicular structures the former showed the higher values in all cases. Comparing the infill factors of parallel and perpendicular structures produced at 56 cm^3/s injection rate and 245 bar backpressure, it can be seen that parallel structures show 25% better infill. At an injection rate of 104 cm3/s and an backpressure of 455 bar, this value is already 28%.

5.1.3. Determination of geometric stiffness due to microstructures

The microstructured surface formed on the polymer products increases the cross-section of the product, thus modifying the "mechanical structure". By calculating the change in inertia of structured products due to excess material using an elementary sample (Figure 7.), the change in mechanical properties can be decomposed into a (quantifiable) component consisting of a change in geometric stiffness and a change in material structure.

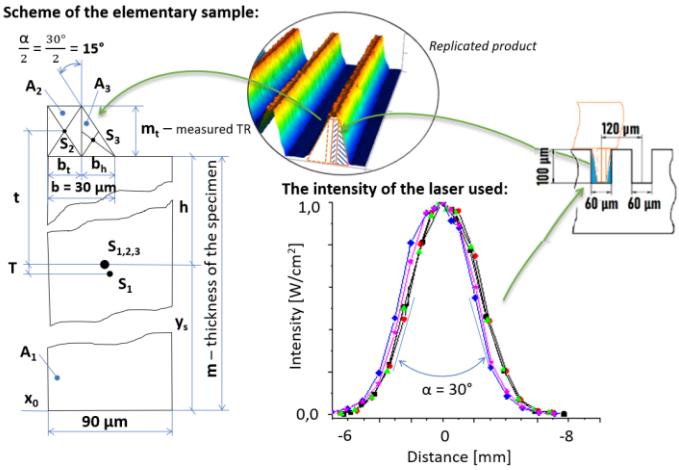

Figure 7. Elementary model used to calculate the change in inertia

Equation to quantify the geometric stiffness (inertia) gain due to the structure:

$$SIV = \left(\frac{I_{S123}}{I_{x1}} \cdot 100\right) - 100\ [\%] \tag{1}$$

5.1.4. Assessment of the bending test results

The experimental plan showed that the injection rate had the greatest effect on the value of the bending forces, so of the 27 experiments (Figure 8) I have shown those where its value varies, while the other two factors are constant.

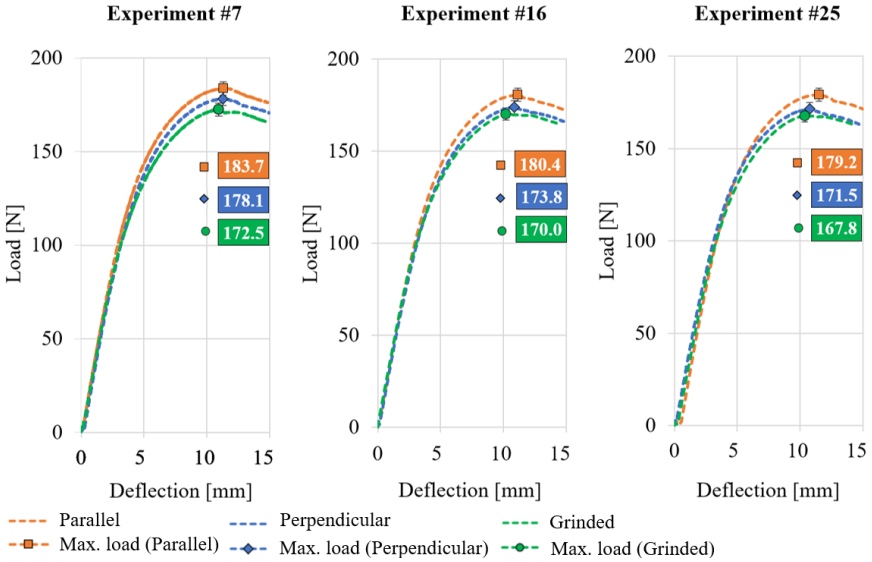

Figure 8. Bending test experiments #7, #16 and #25

In the case of the tested injection moulding parameters, the injection rate and the cooling time reduced the measured maximum bending forces and, through this, the bending strength values. In contrast, the backpressure increased the measured values, which can be explained by the better infill of the product. Products manufactured with different mould surfaces (ground, parallelly structured and perpendicularly structured) produced different bending strength values for the same manufacturing parameters, so the structures have an effect on these mechanical properties of the products.

An increase in flexural strength can be derived from the microstructured surface:

- from the geometric stiffness (inertia) and
- the structural modification of the material.

Based on the relationship in the previous subsection (1), using the structure heights of the products at the time of filling, the percentage form of inertia change and the geometric stiffness gain resulting from their presence can be calculated. The values are given in Table 3:

Table 3. Geometric stiffness gain of parallel and perpendicular structured products

	Parallel structured product replicated 79 µm deep mould cavity			**Vertically structured product replicated 73 µm deep mould cavity**		
	Exp. #7	**Exp. #16**	**Exp. #25**	**Exp. #7**	**Exp. #16**	**Exp. #25**
Height of the structure formed [µm]	43.3	59.5	70.5	28.7	36.7	44.8
TR factor [%]	54.9	75.5	89.5	39.3	50.3	61.3
Change in inertia (Geometric stiffness surplus)	**1.2%**	**1.5%**	**1.7%**	**0.8%**	**1%**	**1.2%**

** The accuracy of the confocal microscope (±0.79 µm) affects the measured values, with a resulting variation of only ±0.02% in percentage terms.*

The flexural strength values calculated from the equation in EN ISO 178 and the percentage differences between them are then summarised in Table 4.

Table 4. Variation of flexural strength values for specimens with different surfaces in 3 experiments

	Flexural strength Exp. #7 [MPa]	Flexural strength Exp. #16 [MPa]	Flexural strength Exp. #25 [MPa]	**Difference due to technological parameters**	
Manufactured with a ground insert	34.0	33.5	33.1	**2.7%**	**avg.: 3%**
Manufactured with perpendicular structure	35.1	34,2	33.8	**3.8%**	
Manufactured with parallel structure	36.2	35,5	35.3	**2.5%**	
Flexural strength increase due to Perpendicular structure [%]	**6.5%**	**6.1%**	**6.8%**		
	average: 6,5%				
Flexural strength increase due to Parallel structure [%]	**3.2%**	**2.2%**	**2.2%**		
	average: 2.5%				

From Table 3, it can be observed that the increase in geometric stiffness due to inertia compared to the products representing the ground surface is up to 1.7% for specimens with parallel structures and 1.2% for those with perpendicular structures. According to the measurements in Table 4, the change in flexural stiffness with parallel microstructures compared to the ground products is on average 6.5%, while for perpendicular structures it is less than half of the latter, on average 2.5%. These results show that the increased flexural strength is influenced not only by the geometrical stiffness (inertia) due to the excess material, but also by the changes in material structure caused by microstructures that modify the flow of the melt. The bending strength was influenced more by the more efficient heat transfer (presence of structures) due to the increased moulding surface area than by the injection rate.

5.1.5. Assessment of the impact test results

The specimens with ground, perpendicular and parallel surface structures are shown in separate diagrams. The diagrams in Figure 9 contain 3 - 3 curves, and each curve shows the results of three different experiments.

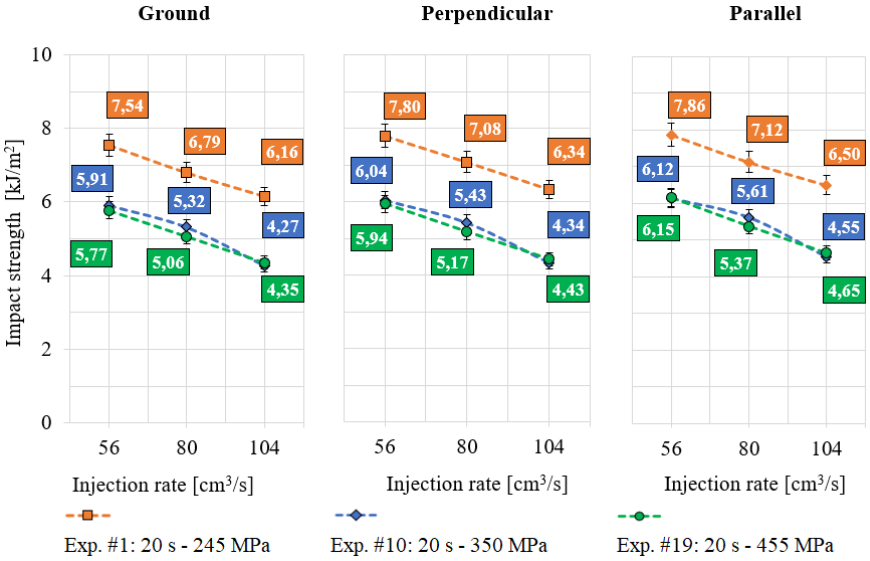

Figure 9. Impact test results for products with ground surface, perpendicular and parallel structured tool inserts

Looking at the diagrams, for all three surface designs, it can be seen that the increase in injection rate is accompanied by a proportional decrease in the impact stregth. Furthermore, it was observed that the highest impact strength values were obtained on the specimens with parallel patterns and the lowest on the specimens with ground surfaces. The percentage differences between the measured values are shown in Table 5.

Table 5. Variation of impact strength values for specimens with different surfaces in 3 experiments

	Impact strength Experiment #1 [kJ/m^2]	Impact strength Experiment #10 [kJ/m^2]	Impact strength Experiment #19 [kJ/m^2]	**Difference due to technological parameters**	
Manufactured with a ground insert	7.54	6.79	6.16	**22.4%**	**average: 22.1%**
Manufactured with perpendicular structure	7.80	7.08	6.34	**23.0%**	
Manufactured with parallel structure	7.86	7.12	6.50	**20.9%**	
Impact strength due to Perpendicular structure [%]	**3.4%**	**4.3%**	**2.9%**		
	average: 3.5%				
Impact strength due to Parallel structure [%]	**4.2%**	**4.9%**	**5.5%**		
	average: 5%				

A comparison of the measured results shows that, in contrast to the bending strength, the technological process parameters of the injection moulding process had a significantly greater effect on the impact strength than the presence of microstructures. The slightly higher impact strength of parallel structures compared to perpendicular structures, similarly to the bending strength is explained by the quality of their infill.

The changes in material structure caused by the geometric stiffness due to the excess material and the change in the flow relationship due to the presence of microstructures in the surface boundary layer increased the impact work by an average of 5% for the parallel-formed structures. Increasing the value of the injection rate resulted in a more rigid behaviour of the specimens, which reduced the impact energy values by 22% on average over the investigated range. The impact energy due to changes in inertia and material structure resulting from the geometry of the surface structures was therefore significantly less than the increase in rigidity caused by increasing the injection rate.

5.2. Assessment of the results of the second set of experiments

In the second set of experiments I investigated the effect of the depth of the structures and started to evaluate the results under the microscope of the prepared moulding inserts. This was followed by an analysis of the surface structures and the effect of the carbon nanotube PP base material on the infill and mechanical properties.

5.2.1. Results of laser surface treatment on the mould inserts

Structures designed to 100 µm were measured to an average depth of 101 µm after production. Structures designed to 20 µm were finished to an average of 22 µm after manufacturing (Figure 10).

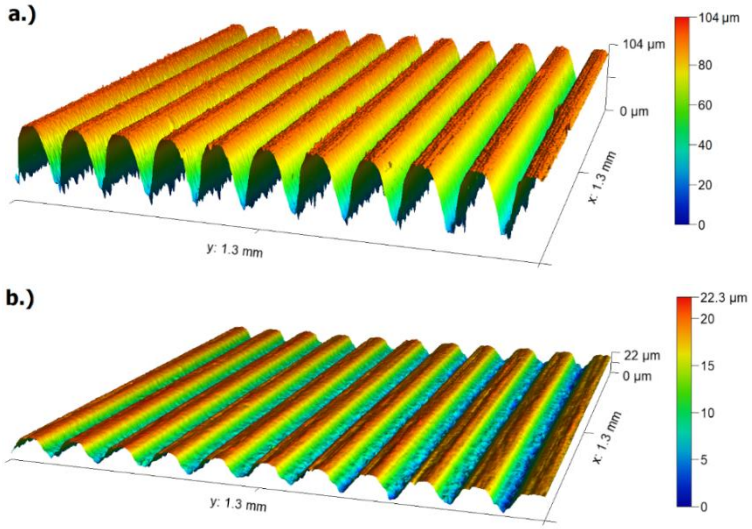

Figure 10. 3D topology of tool inserts with 100 µm (a) and 20 µm (b) deep grooves. Created in Gwyddion software.

The micro-grooves on the inserts **increase the mould surface area, and thus the heat transfer surface area, by 21 ± 0.5% at a depth of 100 µm and by 4.6 ± 0.5% at a depth of 20 µm**. A comparison of the design and the fabricated surface model, and thus the difference between the two, is illustrated in a cross-section in Figure 11.

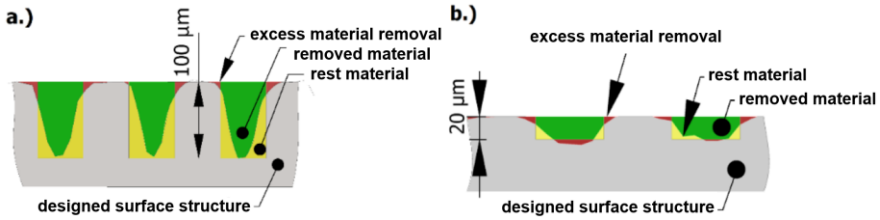

Figure 11. Differences between designed and machined surfaces on tool inserts structured with 100 µm (a) and 20 µm (b) grooves

5.2.2. Results of injection moulded specimen replication

When polypropylene is combined with CNT, the MFI value decreases with increasing reinforcing material mass percentage, which may cause a deterioration of the infill quality. However, in the PP/CNT nanocomposite, recyclation leads to chain unwinding, i.e. degradation, resulting in a decrease in the melt viscosity of the material: the MFI increases. Because of these two opposing effects, I determined the MFI values of the raw materials at the temperatures used before testing the TR factor, which is illustrated in Figure 12.

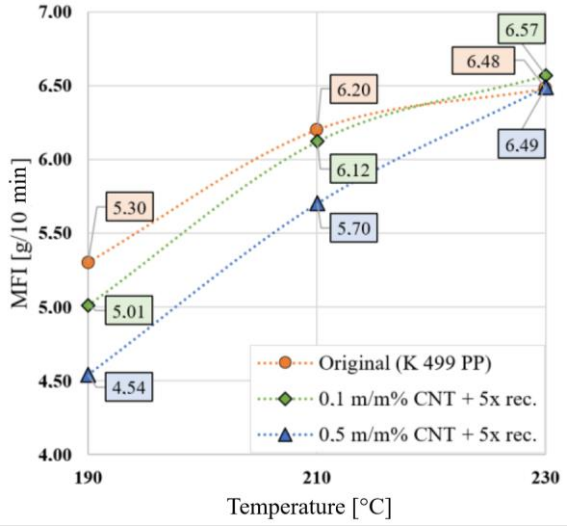

Figure 12. Effect of recycling and CNT content on the MFI values of the original PP raw material and its composites at the investigated temperatures

Based on the main effect analysis of the formation using the **microstructured mould insert with 100 µm grooves**, the melt temperature on the infill is significantly. Furthermore, recyclation and reinforcement phase negatively affect the infill. Shifts in effect lines vary with CNT content. Based on this, when the 100 µm deep structures were formed, the infill was affected differently by CNT content and recycling (Figure 13).

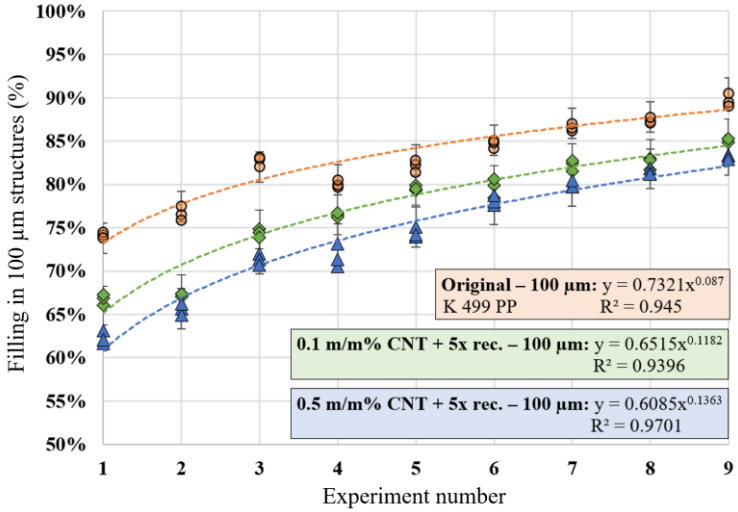

Figure 13. Filling quality of the products of the second set of experiments with 100 µm structures for the three materials tested

From the measurements, it can be concluded that increasing the values of the investigated factors, the infill rate of the recycled CNT-reinforced materials approaches the infill rate of the original material. 0.1 m/m% of carbon nanotubes on average results in a 5% difference and 0.5 m/m% of carbon nanotubes in a 7% difference in the TR factor. The rate of infill further decreases as the mass percentage of the reinforcing phase increases. In Figure 12, the characteristics of the curves plotted on experimental line measurements showing the change in infill compared to the characteristics of the MFI measurements for CNT-enhanced products show a relationship, with the change in flow rates correlating with the infill of structures even in the presence of the reinforcement phase.

A main effect analysis of the moulding of the **microstructured mould insert with 20 µm grooves** showed that both the melt temperature and the backpressure significantly influenced the infill. As a consequence, the interaction of the investigated factors in the experiments is significant.

In contrast to the insert with the 100 µm deep structures, at the 20 µm depth, the lines of action of the recycled CNT-reinforced products are not consistently shifted with respect to the main effect of the original base material. Since the variance is not proportional to the reinforcing phase amount (Figure 13), I concluded that the infill for these materials is more affected by recycling (change in MFI values) than by CNT content.

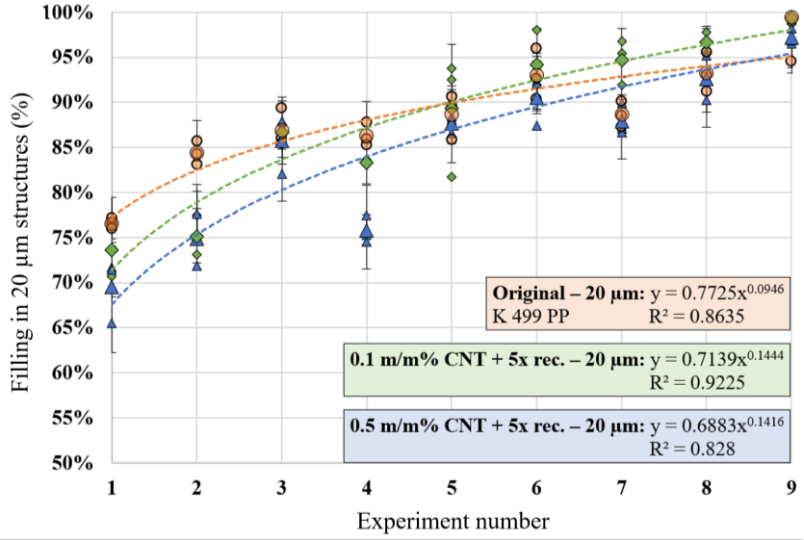

Figure 14. Filling quality of the products of the second series of experiments with 20 µm structures for the three materials tested

The flow properties of the recycled nanocomposite were negatively affected by the reinforcement phase content. The infill rate further decreased with increasing the mass percentage of reinforcement phase. The change in the flow rates due to recyclation is also related to the infill of the structures in the presence of the reinforcement phase.

Increasing the melt temperature and the backpressure can increase the replication. For structures with a depth of 100 µm, the recycled nanocomposite base material could only approach the TR factor values of the original base material with the factors tested. However, the infill quality of the 20 µm deep surface pattern using the recycled nanocomposite base material at 230°C melt temperature and 800 bar backpressure reached 0.5 m/m% CNT and exceeded the infill quality of the original base material at 0.1 m/m%.

5.2.3. Assessment of the tensile test results

I used the tensile test (Figure 15) to select the factors and structures that I analysed using the DMA test.

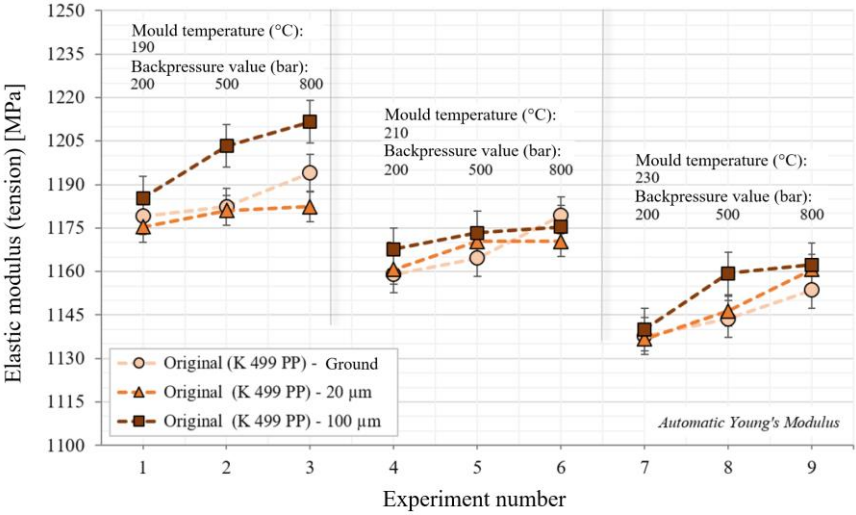

Figure 15. Evolution of elastic modulus values according to experimental settings and surface structures

Significant differences compared to the ground surface (mainly at 190°C melt temperature) were found in the elastic modulus values of the specimens only for structures up to 100 µm. Taking these facts into account, the DMA measurements were carried out only with the change of the melt temperature, while the maximum backpressure was kept constant, for products that have been made using the ground and 100 µm deep grooved inserts.

5.2.4. Assessment of the DMA test results

DMA measurements were used to determine the temperature dependence of the storage modulus (E') and the loss modulus (E"). The storage modulus (the real modulus of elasticity) is the fraction of the test specimen deforming under dynamic loads proportional to the elastically stored energy. In Figure 15, a relaxation indicates the range of phase transitions, (Tg), between 0-20°C.

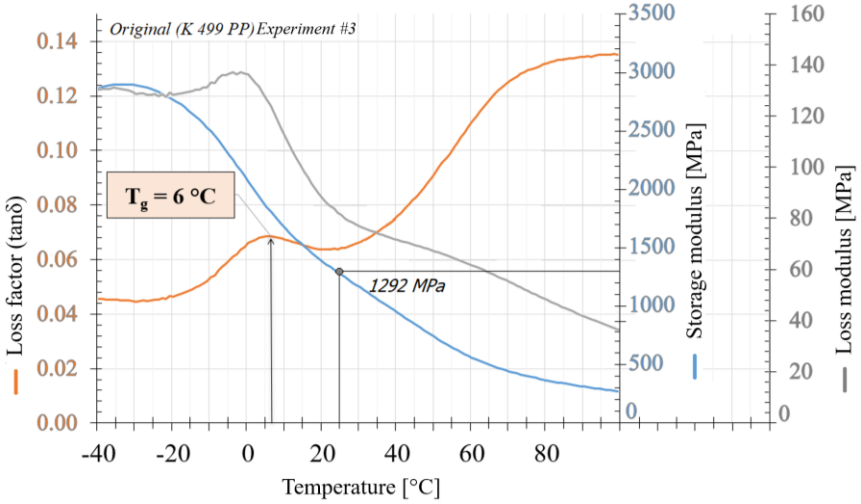

Figure 16. Representation of the loss factor (tanδ) derived from the storage and loss modulus and notation of the glass transition temperature T_g

For rigid solids, the complex modulus is determined primarily by the storage modulus. If tan $\delta \leq 0.1$, then the storage modulus is ≥99% of the complex modulus of elasticity. In this case, the storage modulus from the DMA and the elastic modulus from the static test may be correlated. According to the data sheet for the K 499 PP block copolymer, the tensile modulus of elasticity for this material is 1300 MPa. In Figure 46, it can be observed that the storage modulus value at room temperature is 1292 MPa, which is only 0.6% different from the value given in the data sheet. [46]

In the light of the above findings, the geometric stiffness surplus of specimens representing microstructures was determined (Table 6)

.

Table 6. Geometric stiffness gain of structured products

	Original (K 499 PP) replicated 100 µm deep cavity			0,5 m/m% CNT + 5x rec. replicated 100 µm deep cavity		
	#3	**#6**	**#9**	**#3**	**#6**	**#9**
Height of formed structure [µm]	83.71	85,74	90.78	72.25	79.09	84.21
TR factor [%]	82.70	84,71	89.68	71.38	78.13	83.19
Change in inertia (Geometric stiffness surplus)	**2.4%**	**2.5%**	**2.6%**	**2.2%**	**2.3%**	**2.4%**

Figure 17. shows a comparison of the storage modulus curves (G') of specimens with ground and 100 µm microstructured surfaces in relation to temperature. The measured data validates the tensile test result that the modulus values decrease with increasing melt temperature. This can be explained by the fact that as the temperature increases, the energy content of the molecules increases, intermolecular forces weaken, and as a result, polymer chains are able to move more freely and can assume different conformations. The phenomenon reduces the elastic modulus of the product.

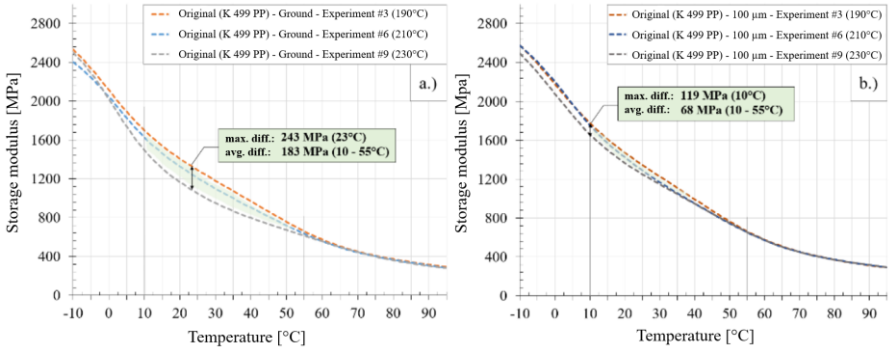

Figure 17. Storage modulus curves (E') of specimens made from the original material, ground (a) and 100 µm structured (b)

According to Figure 17 a.) diagram, it can be observed that the storage modulus values for specimens manufactured and ground at three different melt temperatures varied over a wide range (Figure 17 a.) diagram: mean range 183 MPa) between 10°C and 55°C (marked in green in Figure 17). In contrast, the storage modulus of specimens moulded with a 100 µm structured surface varied significantly over a smaller range (Figure 17 b.) diagram: mean range of 68 MPa) at the investigated melt temperatures. This is because the structured surfaces increase the stiffness of the product over the range investigated thus having a cross effect on the melt temperature. The presence of the structures therefore increases the storage modulus of the specimens, reducing the mean range by 63%.

In order to illustrate the phenomenon more clearly, DMA measurements of specimens with 100 µm surface structures and unstructured specimens at 25°C are compared in Figure 18.

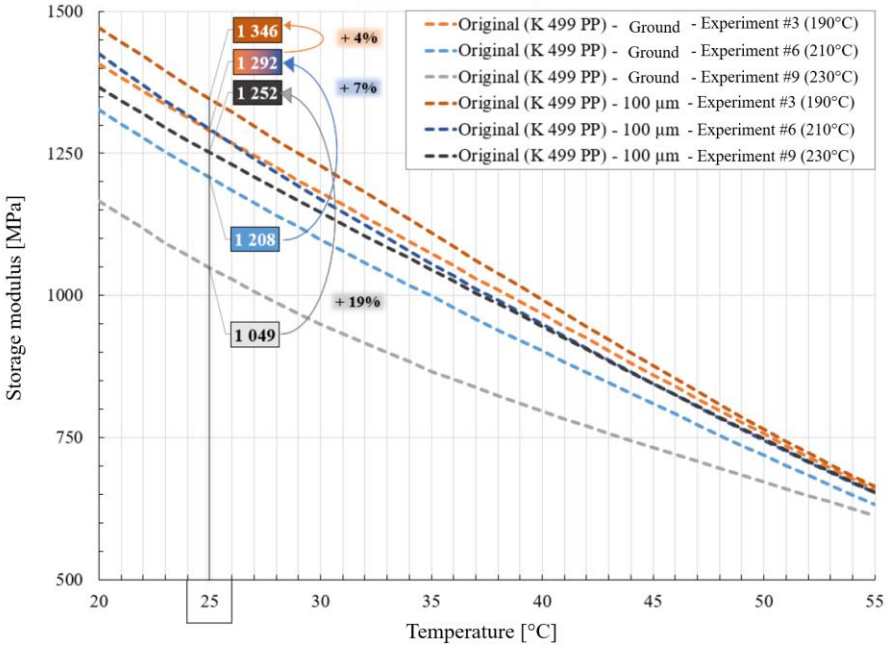

Figure 18. Variation of storage modulus values at 25°C for specimens made of original material, ground and 100 µm structured surface

Based on the plotted values, it can be concluded that, for the same manufacturing parameters, specimens with structure always have a higher storage modulus than specimens with a ground surface (unstructured). At 25°C, it was also observed that structured products resulted in a higher storage modulus even at lower temperatures than their ground counterparts. The presence of 100 µm structures therefore had a greater effect on the change in storage modulus than the values of the melt temperature used in the experiments.

Figure 19 shows the storage modulus curves (e') as a function of temperature for ground and 100 µm structured specimens manufactured from regranulate reinforced with 0.5 m/m% CNT. In Figure 19 (a) diagram, specimens reinforced with CNTs formed on the ground surface varied their storage modulus values over a temperature range between 10°C and 55°C (temperature range of the high elastic state), with a wider average range (Figure 19 (a) diagram: average range 154 MPa) similar to the original material. In contrast, the storage modulus value of specimens with a 100 µm structured surface reinforced with 0.5 m/m% CNT varied in a significantly smaller average range (Figure 19 (b) diagram: average range 65 MPa) at the investigated melt temperatures. The average range has narrowed down by 58% overall.

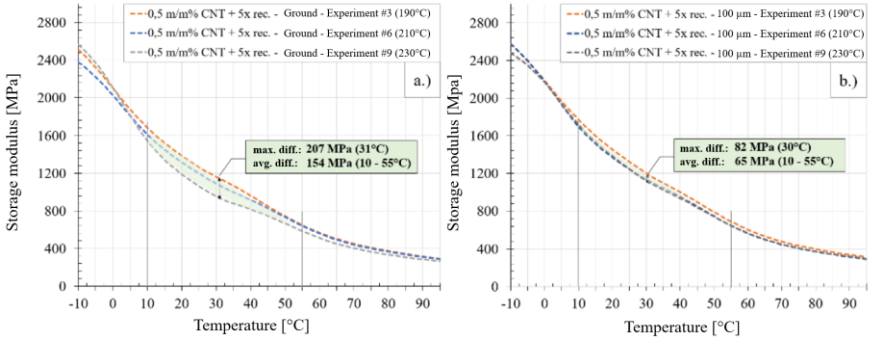

Figure 19. Storage modulus curves (E') of specimens made of PP/CNT composite with ground (a) and 100 µm structured (b) surfaces

As with the original material, I also highlighted the 20-55°C temperature range for the nanocomposite specimens and presented the DMA measurements of the structured and unstructured specimens (Figure 20).

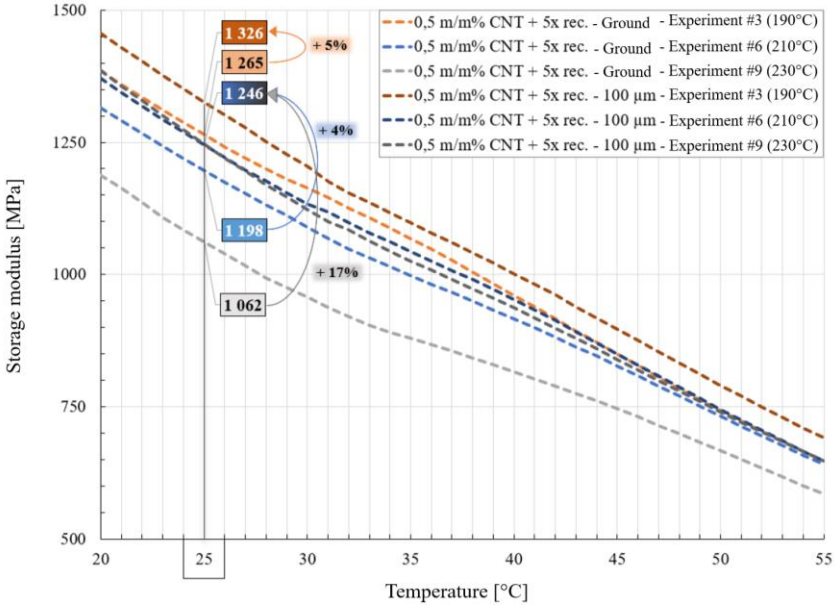

Figure 20. Variation of storage modulus values of specimens made of PP/CNT composite, ground and 100 µm structured surface at 25°C

The increase in modulus values for structured specimens can be explained by the fact that the mapping of microstructures formed on the moulded specimen represents an inertia advantage for the finished product. Furthermore, the structures of the mould surface have an effect on the flow of the polymer melt and, as a consequence of the increased surface area, on the heat transfer ratio. While the former effect may influence the proportion of oriented layers, the latter may influence the proportion of shell structure close to the mould wall and may also affect the crystalline fraction. The exact effect of microstructures on the material structure is very complex due to the above mentioned phenomena, however, from the differences in modulus observed in the measurement results, their presence can be determined by knowing the inertia excess values.

The effect of the microstructure is summarised in Table 7, which shows the variation of the structured surface specimens compared to the ground surface specimens for both the original and the composite in percentage form.

Table 7. Effect of microstructure on mechanical properties

	Original (K 499 PP)				**0,5 m/m% CNT + 5x rec.**			
	Experiment 9.	Experiment 6.	Experiment 3.	9 → 3 [%]	Experiment 9.	Experiment 6.	Experiment 3.	9 → 3 [%]
Storage modulus of ground surface specimens 25 °C-on [MPa]	1049	1208	1292	23	1062	1198	1265	19
Storage modulus of specimens with a 100 µm deep structured surface at 25 °C [MPa]	1252	1292	1346	7,5	1246	1246	1326	6
Storage modulus change [%]	**19%**	**7%**	**4%**		**17%**	**4%**	**5%**	

The table illustrates the effect on the storage modulus of microstructures parallel to the flow of the melt.:

- At a melt temperature of 230°C, the storage modulus of both the unreinforced and the reinforced, reciklated specimens was significantly (17 – 19%) increased.
- The storage modulus of microstructured specimens produced at 230°C melt temperature is only 1.5-3% lower than that of specimens produced at 190°C.
- Replication of the structures at 190°C melt temperature for both unreinforced and reinforced-recycled specimens increased the storage modulus values by 4 – 5%, respectively.

6. Theses - New scientific results

Thesis 1: „I have determined that the filling factor (TR factor) of microstructures formed on the surface of polypropylene random copolymer products using a test injection moulding tool in experiments can be significantly increased by increasing the injection rate. However, the value of the fill factor depends on the orientation of the microstructures relative to the direction of the flow front for the same process parameters. I have shown that at an injection rate of 56 cm^3/s and a backpressure of 245 bar, the filling factor of surfaces structured parallel to the direction to the flow front is 24% better than that of surfaces structured perpendicularly. When tested at an injection rate of 104 cm^3/s and an afterpressure of 455 bar, a difference of 28% is observed. This phenomenon can be explained by the more favourable flow conditions." [S1-S3, S6, S9, S10, S13, S14]

Thesis 2: „I have determined that during injection moulding, microstructures replicating on the surface of a random polypropylene copolymer specimen parallel to the direction of the flow front can increase the flexural strength. I have verified by measurements and calculation that the increase is due to the geometric stiffness (inertia) resulting from the excess material and to the changes in material structure caused by microstructures affecting the flow of the melt." [S1, S3, S6, S13]

Thesis 3: „I have determined that the specific impact strength of injection moulded polypropylene random copolymer specimens was less affected by the presence of microstructures on the moulding surface of the injection mould than by the more brittle behaviour with increasing injection rate. I have shown that, at the process parameters used (injection rate: 104 cm^3/s, backpressure: 455 bar), microstructures formed parallel to the direction of the flow front increase the specific impact strength of the specimen by an average of 5% compared to the specimen without structures. In contrast, increasing the injection rate (from 56 cm^3/s to 104 cm^3/s) reduces the specific impact strength by 22% on average." [S1, S3, S6, S13]

Thesis 4: „I have determined that the replication of microstructures formed parallel to the direction of the flow front in injection moulding of recycled polypropylene nanocomposite containing carbon nanotubes is differently influenced by the mass fraction of the reinforcing phase and the depth of the structures. I have shown that the variation of the melt flow index of recycled polypropylene nanocomposites containing 0.1 m/m% and 0.5 m/m% carbon nanotubes correlates with the filling factor (TR factor) of the microstructures formed on the surface of the products manufactured at the investigated melt temperatures (190°C, 210°C, 230°C).”
[S1-S3, S5-S6, S9-10, S13-S14]

Thesis 5: „I have determined that microstructures replicated on the surface of injection-moulded polypropylene block copolymer and recycled nanocomposite specimens parallel to the direction of the flow front increase the storage modulus values of the product. I have shown that the storage modulus of specimens with 100 μm deep structured surfaces at 25°C, manufactured at 230°C melt temperature, is 19% higher for polypropylene block copolymer and 17% higher for recycled polypropylene with 0.5 m/m% carbon nanotube content than for specimens without structures. This phenomenon can be explained by a combination of geometric stiffness and material structure changes caused by microstructures.”
[S1, S3, S6, S8, S12].

7. List of the publications related to the PhD research

S1 K. Kun, Z. Weltsch, Effect of femtosecond laser structured injection moulding tool on mechanical properties of the manufactured product, Polymers 2021, 13, 2187. IF=4,967 Q1 https://doi.org/10.3390/polym13132187

S2 K. Kun, J. Líska, Z. Weltsch, Replication of microstructures formed by femtosecond laser during injection moulding, Advances in Manufacturing Engineering and Materials II ; Springer International Publishing (2021) pp. 290-300. Paper: Chapter 24 , 11 p

S3 K. Kun, Z. Weltsch, Research of the effect of macrogeometric structures on the melt front using simulation, Advances in Manufacturing Engineering and Materials II ; Springer International Publishing (2021) pp. 282-289. Paper: Chapter 23 , 8 p

S4 J. Líska, K. Kun. Zs. Kovács, Attendants at MMC composite milling, Advances in Manufacturing Engineering and Materials II ; Springer International Publishing (2021) pp. 332-342. Paper: Chapter 27 , 11 p.

S5 K. Kun, Design of an Experimental Injection Moulding Tool for Testing Microstructured Cavity Surfaces. Acta Materialia Transylvanica, (2021). 4(2), 97-102.

S6 K. Kun, P. Boza, Investigation of inserts surface structures on injection moulded parts. In: IOP Conference Series: Materials Science and Engineering. IOP Publishing, 2018. p. 012052.

S7 J. Líska, K. Kun, K. Líska, MMC materials ultrasonic machining and its economic aspects. Procedia Engineering, 2016, 149: 245-256

S8 K. Kun, A. Bata, Újrahasznosított, CNT-vel erősített PP kompozitok mikroszerkezeti vizsgálata konfokális mikroszkóppal GRADUS Vol 10, No 1 (2023.) ISSN: 2064-8014 (megjelenés alatt)

S9 K. Kun, Z. Weltsch, J. Líska, Femtoszekundumos lézerrel felületkezelt fröccsöntő szerszámbetét termékének vizsgálata GRADUS 9 : 2 Paper: 2022.2.ENG.002 , 7 p. (2022)

S10 K. Kun, P. Boza, Z. Weltsch, Polimer ömledék leképeződésének vizsgálata formaüreg felületi struktúráin GRADUS 6 : 1 pp. 142-147. Paper: 18 , 6 p. (2019)

S11 K. Kun, Technológiai paraméterek hatása Digital Lighting Process eljárásnál GRADUS, 7 (2). (2020) pp. 374-379.

S12 L. Ihász, K. Kun, Újrahasznosított, CNT-vel erősített PP kompozitok mikroszerkezeti vizsgálata Neumann János Egyetem TDK, Polimer szekció (2023)

S13 A. Bognár, K. Kun, Femtoszekundumos lézerrel létrehozott mikrostruktúrák hatása polimer termékek mechanikai tulajdonságaira 35 OTDK, Műszaki Tudományi Szekció, Polimer anyagtudomány és vizsgálat Tagozat. 2021.

S14 K. Kun, P. Boza, Z. Weltsch, Felületi struktúrák vizsgálata fröccsöntő szerszám betéteken AGTEDU 2018, Kecskemét: 2018. november 15., Presemtation

S15 K. Kun, Z. Weltsch, Felületi struktúrák vizsgálata szimuláció segítségével AGTEDU 2018, Kecskemét: 2018. november 15., Presentation

8. References

[1] Bánhegyi György, “A mikrofröccsöntés jelene és lehetőségei,” *Műanyagipari szemle - Műanyagok feldolgozása*, vol. 5, pp. 1–9, 2006.

[2] K. , B. P. , & P. M. Belina, “Investigation of the effect of surface finishing on injection moulding parts,” in *11th International conference on tools*, Miskolc, Hungary, 2004, pp. 311–316.

[3] Bulk Chemicals, “Automotive Plastics Market Size, Share & Trends Analysis Report,” 2021.

[4] ASTM D883-19, “Standard Terminology Relating to Plastics,” 2019

[5] B. Sha, S. Dimov, C. Griffiths, and M. S. Packianather, “Investigation of micro-injection moulding: Factors affecting the replication quality,” *J Mater Process Technol*, vol. 183, no. 2–3, pp. 284–296, Mar. 2007, doi: 10.1016/j.jmatprotec.2006.10.019.

[6] D. Masato, L. Piccolo, G. Lucchetta, and M. Sorgato, “Texturing Technologies for Plastics Injection Molding: A Review,” *Micromachines (Basel)*, vol. 13, no. 8, p. 1211, Jul. 2022, doi: 10.3390/mi13081211.

[7] A. Zoubir, L. Shah, K. Richardson, and M. Richardson, “Practical uses of femtosecond laser micro-materials processing,” *Applied Physics A*, vol. 77, no. 2, pp. 311–315, Jul. 2003, doi: 10.1007/s00339-003-2121-9.

[8] M. Dantus, *Dantus, Marcos. Femtosecond Laser Shaping: From Laboratory to Industry*. CRC Press, 2017.

[9] Z. Lin and M. Hong, “Femtosecond Laser Precision Engineering: From Micron, Submicron, to Nanoscale,” *Ultrafast Science*, vol. 2021, Jan. 2021, doi: 10.34133/2021/9783514.

[10] X.-Q. Liu, B.-F. Bai, Q.-D. Chen, and H.-B. Sun, “Etching-assisted femtosecond laser modification of hard materials,” *Opto-Electronic Advances*, vol. 2, no. 9, pp. 19002101–19002114, 2019, doi: 10.29026/oea.2019.190021.

[11] L. Calabrese *et al.*, “Micro-Milling Process of Metals: A Comparison between Femtosecond Laser and EDM Techniques,” *Journal of Manufacturing and Materials Processing*, vol. 5, no. 4, p. 125, Nov. 2021, doi: 10.3390/jmmp5040125.

[12] L. Yang, W. Ma, F. Gao, and S. Xi, “Effect of EDM and Femtosecond-Laser Groove-Texture Collision Frequency on Tribological Properties of 0Cr17Ni7Al Stainless Steel,” *Coatings*, vol. 12, no. 5, p. 611, Apr. 2022, doi: 10.3390/coatings12050611.

[13] S. S. Wangikar, P. K. Patowari, and R. D. Misra, “Parametric Optimization for Photochemical Machining of Copper Using Grey Relational Method,” in *Techno-Societal 2016*, Cham: Springer International Publishing, 2018, pp. 933–943. doi: 10.1007/978-3-319-53556-2_94.

[14] M. N. W. Groenendijk and J. Meijer, “Surface Microstructures obtained by Femtosecond Laser Pulses,” *CIRP Annals*, vol. 55, no. 1, pp. 183–186, 2006, doi: 10.1016/S0007-8506(07)60394-1.

[15] A. Gruner, J. Schille, and U. Loeschner, “Experimental Study on Micro Hole Drilling Using Ultrashort Pulse Laser Radiation,” *Phys Procedia*, vol. 83, pp. 157–166, 2016, doi: 10.1016/j.phpro.2016.08.030.
[16] T. Hanemann, W. Pfleging, J. Haußelt, and K.-H. Zum, “Laser micromaching and light induced reaction injection molding as suitable process sequence for the rapid fabrication of microcomponents,” *Microsystem Technologies*, vol. 7, no. 5–6, pp. 209–214, Jan. 2002, doi: 10.1007/s005420100116.
[17] U. A. Theilade and H. N. Hansen, “Surface microstructure replication in injection molding,” *The International Journal of Advanced Manufacturing Technology*, vol. 33, no. 1–2, pp. 157–166, May 2007, doi: 10.1007/s00170-006-0732-y.
[18] Yao Donggang, “Injection molding high aspect ratio microfeatures,” *Journal of injection molding technology*, vol. 6, no. 1, pp. 1–11, 2002.
[19] U. M. Attia and J. R. Alcock, “An evaluation of process-parameter and part-geometry effects on the quality of filling in micro-injection moulding,” *Microsystem Technologies*, vol. 15, no. 12, pp. 1861–1872, Dec. 2009, doi: 10.1007/s00542-009-0923-1.
[20] U. M. Attia, S. Marson, and J. R. Alcock, “Micro-injection moulding of polymer microfluidic devices,” *Microfluid Nanofluidics*, vol. 7, no. 1, pp. 1–28, Jul. 2009, doi: 10.1007/s10404-009-0421-x.
[21] H.-C. Chang and W.-B. Young, “Experimental Study on the Filling of a Micro Injection Molding with Cylindrical Dot Patterns,” *International Polymer Processing*, vol. 20, no. 3, pp. 245–249, Sep. 2005, doi: 10.3139/217.1884.
[22] R. Pantani, A. Sorrentino, V. Speranza, and G. Titomanlio, “Molecular orientation in injection molding: experiments and analysis,” *Rheol Acta*, vol. 43, no. 2, pp. 109–118, Mar. 2004, doi: 10.1007/s00397-003-0325-8.
[23] J. Ying, X. Xie, S. Peng, H. Zhou, and D. Li, “Morphology and rheology of PP/POE blends in high shear stress field,” *Journal of Thermoplastic Composite Materials*, vol. 31, no. 9, pp. 1263–1280, Sep. 2018, doi: 10.1177/0892705717734908.
[24] V. V. Zuev, B. Steinhoff, S. Bronnikov, H. Kothe, and I. Alig, “Flow-induced size distribution and anisotropy of the minor phase droplets in a polypropylene/poly (ethylene-octene) copolymer blend: Interplay between break-up and coalescence,” *Polymer (Guildf)*, vol. 53, no. 3, pp. 755–760, Feb. 2012, doi: 10.1016/j.polymer.2011.12.046.
[25] C. Gornik, “Injection Moulding of Parts with Microstructured Surfaces for Medical Applications,” *Macromol Symp*, vol. 217, no. 1, pp. 365–374, Oct. 2004, doi: 10.1002/masy.200451332.
[26] K. Porfyrakis, H. E. Assender, and I. M. Robinson, “The interrelationship between processing conditions, microstructure and mechanical properties for injection moulded rubber-toughened poly(methyl methacrylate)

(RTPMMA) samples," *Polymer (Guildf)*, vol. 43, no. 17, pp. 4769–4781, Aug. 2002, doi: 10.1016/S0032-3861(02)00286-0.
[27] N. Solomon, I. Solomon, and E. Sanduleac, "Material flow influence on the quality of molded parts," *Polymer Bulletin*, vol. 76, no. 11, pp. 5981–6000, Nov. 2019, doi: 10.1007/s00289-019-02832-w.
[28] Ferenc Ronkay, "Effect of Recycling on the Rheological, Mechanical and Optical Properties of Polycarbonate," *Acta Polytechnica Hungarica*, vol. 10, no. 1, pp. 209–220, 2013.
[29] L. Lendvai *et al.*, "Development and characterization of composites produced from recycled polyethylene terephthalate and waste marble dust," *Polym Compos*, vol. 43, no. 6, pp. 3951–3959, Jun. 2022, doi: 10.1002/pc.26669.
[30] C. S. Grimmer and C. K. H. Dharan, "High-cycle fatigue of hybrid carbon nanotube/glass fiber/polymer composites," *J Mater Sci*, vol. 43, no. 13, pp. 4487–4492, Jul. 2008, doi: 10.1007/s10853-008-2651-9.
[31] R. Ashok Gandhi, V. Jayaseelan, K. Palani Kumar, B. K. Raghunath, and S. Krishnaraj, "Effect of Carbon Nano Tubes (CNT) on Hardness of Polypropylene Matrix," 2019, pp. 261–270. doi: 10.1007/978-981-13-1780-4_26.
[32] J. Zhang *et al.*, "The effects of recycling on the properties of carbon nanotube-filled polypropylene composites and worker exposures," *Environ. Sci.: Nano*, vol. 3, no. 2, pp. 409–417, 2016, doi: 10.1039/C5EN00253B.
[33] K. Zdiri, A. Elamri, M. Hamdaoui, O. Harzallah, N. Khenoussi, and J. Brendlé, "Reinforcement of recycled PP polymers by nanoparticles incorporation," *Green Chem Lett Rev*, vol. 11, no. 3, pp. 296–311, Jul. 2018, doi: 10.1080/17518253.2018.1491645.
[34] R. Samad, L. Courrol, S. Baldochi, and N. Vieir, "Ultrashort Laser Pulses Applications," in *Coherence and Ultrashort Pulse Laser Emission*, InTech, 2010. doi: 10.5772/13095.
[35] J. Preußner, S. Oeser, W. Pfeiffer, A. Temmler, and E. Willenborg, "Microstructure and Residual Stresses of Laser Structured Surfaces," *Adv Mat Res*, vol. 996, pp. 568–573, Aug. 2014, doi: 10.4028/www.scientific.net/AMR.996.568.
[36] A. K. Dubey and V. Yadava, "Laser beam machining—A review," *Int J Mach Tools Manuf*, vol. 48, no. 6, pp. 609–628, May 2008, doi: 10.1016/j.ijmachtools.2007.10.017.
[37] K. Maghsoudi, R. Jafari, G. Momen, and M. Farzaneh, "Micro-nanostructured polymer surfaces using injection molding: A review," *Mater Today Commun*, vol. 13, pp. 126–143, Dec. 2017, doi: 10.1016/j.mtcomm.2017.09.013.
[38] F. Modica, V. Basile, R. Surace, and I. Fassi, "Replication Study of Molded Micro-Textured Samples Made of Ultra-High Molecular Weight

Polyethylene for Medical Applications," *Micromachines (Basel)*, vol. 14, no. 3, p. 523, Feb. 2023, doi: 10.3390/mi14030523.

[39] A.-K. Holthusen, O. Riemer, J. Schmütz, and A. Meier, "Mold machining and injection molding of diffractive microstructures," *J Manuf Process*, vol. 26, pp. 290–294, Apr. 2017, doi: 10.1016/j.jmapro.2017.02.014.

[40] D. Masato, M. Sorgato, and G. Lucchetta, "Analysis of the influence of part thickness on the replication of micro-structured surfaces by injection molding," *Mater Des*, vol. 95, pp. 219–224, Apr. 2016, doi: 10.1016/j.matdes.2016.01.115.

[41] H. Yokoi, X. Han, T. Takahashi, and W. K. Kim, "Effects of molding conditions on transcription molding of microscale prism patterns using ultra-high-speed injection molding," *Polym Eng Sci*, vol. 46, no. 9, pp. 1140–1146, Sep. 2006, doi: 10.1002/pen.20519.

[42] D. Tabuani, W. Granelli, G. Camino, and M. Claes, "Polypropylene based carbon nanotubes composites: structure and properties," *e-Polymers*, vol. 8, no. 1, Dec. 2008, doi: 10.1515/epoly.2008.8.1.1178.

[43] Industrial-Grade Femtosecond Lasers: Monaco 1035 | Coherent prospect
https://content.coherent.com/legacy-assets/pdf/COHR_Monaco1035_DS_0120_1.pdf
Seen: 2023.04.01.

[44] Cavity Eye – Pressure Monitoring
https://cavityeye.com/
Seen: 2023.04.01.

[45] Tatren RM 85 82 Clear PP random kopolimer – Technical datasheet
https://www.molgroupchemicals.com/userfiles/products/80/80_tds_hu.pdf
Seen: 2023.04.01.

[46] Tippelen K 499 PP blokk kopolimer
https://mol.hu/images/mol_hu/pdf/vallalati_ugyfelek/polimer-termekek/termekek/pp-polipropilenek/tipplen/tipplen_k_499_hu_2018.pdf
Seen: 2023.04.01.

[47] Nanocyl NC7000 MWCNT – Technical datasheet
https://www.nanocyl.com/wp-content/uploads/2016/07/DM-TI-02-TDS-NC7000-V08.pdf
Seen: 2023.04.01

[48] Wittmann Battenfeld Ecopower 55 – Catalogue
https://www.wittmann-group.com/sites/default/files/2022-09/ecopower_en_2022-08_web.pdf
Seen: 2023.04.01

[49] Olympus OLS500 – SAF Confocal Microscopy catalogue
https://unicam.hu/files/olympus-lext-ols5100/LEXT-OLS5100_prospektus.pdf
Seen: 2023.04.01